Available online at www.sciencedirect.com
ScienceDirect
Geochimica et Cosmochimica Acta 74 (2010) 4110–4122
Geochimica et Cosmochimica Acta
www.elsevier.com/locate/gca

Clumped isotope thermometry of carbonatites as an indicator of diagenetic alteration

Kate J. Dennis *, Daniel P. Schrag

Department of Earth and Planetary Sciences, Harvard University, 20 Oxford Street, Cambridge, MA 02138, USA

Received 16 September 2009; accepted in revised form 6 April 2010; available online 24 April 2010

Abstract

We measure the clumped isotopic signature of carbonatites to assess the integrity of the clumped isotope paleothermometer over long timescales (10^7–10^9 years) and the susceptibility of the proxy to closed system re-equilibration of isotopes during burial diagenesis. We find pristine carbonatites that have primary oxygen isotope signatures, along with a Carrara marble standard, do not record clumped isotope signatures lighter than 0.31‰ suggesting atoms of carbon and oxygen freely exchange within the carbonate lattice at temperatures above 250–300 °C. There is no systematic trend in the clumped isotope signature of pristine carbonatites with age, although partial re-equilibration to lower temperatures can occur if a carbonatite has been exposed to burial temperatures for long periods of time. We conclude that the solid-state re-ordering of carbon and oxygen atoms is sufficiently slow to enable the use of clumped isotope paleothermometry on timescales of 10^8 years, but that diagenetic resetting can still occur, even without bulk recrystallization. In addition to the carbonatite data, an inorganic calibration of the clumped isotope paleothermometer for low temperature carbonates (7.5–77 °C) is presented and highlights the need for further inter-lab standardization.

1. INTRODUCTION

Clumped isotope geochemistry has great potential for enabling the reconstruction of temperatures in ancient systems due to the isotopic independence of a carbonate mineral's clumped isotopic signature from the water in which it precipitated. The thermometer is based on the single-phase mass-dependent isotope exchange reaction between individual metal-carbonate molecules (e.g., $CaCO_3$) that increasingly promotes the 'clumping' of heavy isotopes into a single carbonate ion as temperature decreases. This drive for clumping at low temperatures is used to form the basis of a carbonate clumped isotope paleothermometer, a measure of the deviation in doubly-substituted isotopologues of acid-derived CO_2 (predominantly $^{13}C^{18}O^{16}O$) from that expected if all isotopes were randomly distributed among the isotopologues (Ghosh et al., 2006b; Eiler, 2007). Empirical calibrations and modern natural carbonates have been shown to conform to the thermodynamic principle expected for multiply-substituted ('clumped') isotopologues of the carbonate ion (Ghosh et al., 2006b; Eiler, 2007; Eiler et al., 2009).

The utility of clumped isotopes in reconstructing ancient temperatures may be complicated by solid-state exchange of oxygen and carbon atoms within the carbonate lattice resulting in the re-ordering of isotopologues and a re-equilibration at burial temperatures without open-system exchange of isotopes. These molecular-scale processes are important because the clumped isotope proxy is based on the ordering of O and C atoms within the carbonate mineral lattice, and therefore, diagenetic alteration can occur via bulk recrystallization and/or molecular scale exchange of O and C atoms within the solid-state crystal lattice. In the first case, the bulk isotopic composition ($\delta^{13}C$ and/or $\delta^{18}O$) and the clumped isotopic signature (Δ_{47}) of the carbonate mineral is altered assuming the water to rock ratio is high, and the isotopic composition of the water is very different from the initial source water, while in the second

* Corresponding author. Tel.: +1 617 384 8398.
E-mail address: kdennis@fas.harvard.edu (K.J. Dennis).

0016-7037/$ - see front matter © 2010 Elsevier Ltd. All rights reserved.
doi:10.1016/j.gca.2010.04.005

case only the clumped isotope signature will change. As a result, solid-state exchange of isotopes might impose a limit on how far back in time one can use the carbonate clumped isotope paleothermometer.

While clumped isotope paleothermometry has been used to analyze CM chondrites (Guo and Eiler, 2007) and samples from the Pleistocene (Affek et al., 2008), Miocene (Ghosh et al., 2006a) and Paleozoic (Came et al., 2007), no study has thoroughly assessed the integrity of the clumped isotope proxy over long (10^7–10^9 years) timescales. In this paper, the clumped isotope paleothermometer is applied to a suite of carbonatite rocks which are used as a geologic test for the integrity of the proxy over millions of years.

1.1. Theory of clumped isotope paleothermometry

A brief overview of carbonate clumped isotope paleothermometry is presented. For a more detailed discussion of the broader field of clumped isotope geochemistry, see Eiler (2007).

Clumped isotope paleothermometry is quantified using the metric Δ_{47}, a measure of the deviation in mass 47 CO_2 (predominantly $^{13}C^{18}O^{16}O$) from that expected if isotopes were randomly distributed (Eq. (1)), where R_{47} is the ratio of mass 47 to mass 44 CO_2 measured in the sample and R^*_{47} is the ratio of mass 47 to mass 44 CO_2 expected in the sample if all isotopes of O and C were randomly distributed among the different isotopologues (the 'stochastic' distribution).

$$\Delta_{47} = \left(\frac{R_{47}}{R^*_{47}} - 1\right) \times 1000\ (‰) \tag{1}$$

The CO_2 used to quantify Δ_{47} is produced by acid digestion of a carbonate mineral, and as the temperature of formation of a carbonate mineral decreases the Δ_{47} metric increases. This is because the zero-point energy differences between isotopologues of the carbonate ion result in multiply-substituted isotopologues being more stable (lower zero-point energy) than isotopologues with zero or one heavy isotope (higher zero-point energy). At high temperatures, the competing effect of entropy promotes disorder in the system and a random distribution of isotopologues. Therefore at low temperature, carbonate minerals have more doubly-substituted isotopologues than would be expected if all isotopes were randomly distributed among the isotopologues.

The original calibration of the clumped isotope thermometer used inorganic calcite precipitated at controlled temperatures between 1 and 50 °C to determine the relationship between temperature of $CaCO_3$ precipitation and Δ_{47} (Ghosh et al., 2006b; Eq. (2)). Since the proxy measures deviations in low abundance isotopologues of CO_2 ($^{13}C^{18}O^{16}O = 44$ ppm) parts per million precision is required to accurately interpret the proxy ($\pm 0.005‰$ resolves ±1 °C at earth's surface temperatures).

$$\Delta_{47} = \frac{0.0592 \times 10^6}{T^2} - 0.02 \tag{2}$$

For higher temperature applications, a theoretical calculation (Guo et al., 2009) based on transition state theory, statistical thermodynamics, ^{13}C–^{18}O clumping in carbonate minerals and the fractionation associated with acid digestion is used to describe the relationship between temperature and Δ_{47}:

$$\Delta_{47} = -\frac{3.33040 \times 10^9}{T^4} + \frac{2.32415 \times 10^7}{T^3} - \frac{2.91282 \times 10^3}{T^2} - \frac{5.54042}{T} + 0.23252 \tag{3}$$

Eqs. (2) and (3) show Δ_{47} is a function of temperature only, and, unlike the oxygen isotope paleothermometer, it is independent of the isotopic composition of the solution from which the carbonate precipitated. This single-phase property makes the clumped isotope proxy accessible to geologic problems where little is known about the coexisting phase. For example, the proxy could be used to reconstruct terrestrial temperature records or to deconvolve temperature signals from ice volume signals in the $\delta^{18}O$ of marine carbonates.

1.2. Solid-state diffusion and the clumped isotope paleothermometer

Unlike other proxies, for example $\delta^{18}O$ and $\delta^{13}C$, where open system macro-recrystallization alters the geochemical signature, alteration of the clumped isotope signature could also occur in a closed system and on the molecular scale with no change in bulk isotopic signature. Therefore, an understanding of the rate of solid-state diffusion of O and C within the carbonate lattice is required. If solid-state diffusion is sufficiently fast at burial temperatures to allow exchange of O and C within the carbonate lattice, the clumped isotope proxy could be compromised over geologic timescales and the Δ_{47} value measured may not represent the crystallization or precipitation temperature, but some burial temperature or a combination of both.

Using the characteristic scaling between diffusivity (D), time (t) and distance of diffusion (x): $x = \sqrt{Dt}$, and assuming the critical diffusion length scale for the clumped isotope proxy is the length of a unit cell of calcite (5 Å), it is possible to obtain an estimate of the rate of diffusion above which the primary clumped isotope signature could be compromised. Rates of diffusion between 10^{-29} and 10^{-32} $cm^2\ s^{-1}$ could result in solid-state exchange of isotopes across the unit cell of calcite over 10^6 to 10^9 years.

Experiments aimed at determining the solid-state diffusion coefficients of O and C in calcite have been conducted at high temperatures (Anderson, 1969, 1972; Kronenberg et al., 1984; Farver, 1994; Labotka et al., 2004) but due to slow rates of diffusion, few experiments have been conducted at lower than 600 °C and we are aware of only one conducted at 400 °C (Farver, 1994). In general, bulk exchange and ion microprobe experiments yield similar results with O diffusivity increasing from 10^{-18} to 10^{-13} $cm^2\ s^{-1}$ and C diffusivity increasing from 10^{-19} to 10^{-14} $cm^2\ s^{-1}$ for temperatures from 400 to 850 °C (Anderson, 1969, 1972; Kronenberg et al., 1984; Farver, 1994; Labotka et al., 2004). The rate of diffusion of C is predominantly controlled by temperature, while the diffusivity of O has a complex dependence on temperature, water fugacity, CO_2 partial pressure and the purity of calcite. The range in diffusivities of O and C are shown in

Fig. 1, but as discussed below, extrapolating these high temperature experimental results to geologically significant diagenetic temperatures only provide us with low confidence estimates of diffusivity.

First, although the majority of work suggests a linear Arrhenian relationship between temperature and the log of diffusivity (e.g., Anderson, 1969, 1972; Kronenberg et al., 1984; Labotka et al., 2004) the data of Farver (1994) suggests the diffusivity of O may be concave with temperature due to the effect of water fugacity (dark grey triangles in Fig. 1), while Kronenberg et al. (1984) find the diffusion of O, when normalized to $pH_2O = 0.1$ MPa, does not fit an Arrhenius relationship over 500 and 800 °C, possibly due to impurities in the calcite mineral structure. A potential explanation for non-Arrhenian behavior could be that the dominant mechanisms controlling the diffusivity of O change with temperature regime. Second, the environmental pressure and water content surrounding the mineral can significantly change the rate of diffusion. Anderson (1972) finds that the diffusivity of O is accelerated by an order of magnitude under high CO_2 pressure ($pCO_2 = 82.5$ MPa compared to $pCO_2 = 10$ MPa), while Kronenberg et al. (1984) find O diffusion is enhanced by high Mn concentrations (Mn-rich calcite with 1180 ppm Mn accelerates diffusion by a factor of ~5 compared to high purity calcite with 100 ppm Mn) and high H_2O pressure (up to $pH_2O = 2.4$ MPa). Farver (1994) finds O diffusion rates have a strong positive correlation with water fugacity between 10 and 350 MPa and suggest water is the dominant transport species for O in calcite. Third, the defect structure of a mineral may play an important role in controlling the rate of diffusion as shown by lower diffusion coefficients in annealed materials (Anderson, 1969; Farver, 1994), and by the enhancement of O diffusion in Mn-rich calcite (Kronenberg et al., 1984).

Due to the above complexities in understanding the rate of C and O solid-state diffusion, low confidence exists in our ability to extrapolate experimentally determined diffusion coefficients to burial temperatures. This is particularly significant for O diffusion because of the control factors other than temperature, e.g., the partial pressure of CO_2 and H_2O, and mineral impurities, have on the rate of solid-state exchange. Therefore, we propose a geologic test using carbonatites to empirically study solid-state diffusion within the carbonate lattice.

1.3. Carbonatites as a geologic test

Carbonatites are igneous rocks composed of greater than 50% carbonate minerals. There are two main hypotheses for their formation (i) primary melting of carbonated peridotite (Bell et al., 1998; Harmer and Gittins, 1998) and (ii) partial melting and differentiation from carbonated silicate melts (Burke and Khan, 2006). Primary melting of carbonated peridotite is thought to occur in the mantle at depths greater than 70 km giving a high temperature and pressure formation regime, while differentiation from carbonated silicate melts likely occurs within the shallow mantle or crust. Evidence for high temperature crystallization regimes (ca. 550–900 °C) from calcite–dolomite geothermometry and oxygen isotope fractionations between calcite and associated silicate minerals (Gittins, 1979; Haynes et al., 2003), along with the mantle-like Sr and Nd signatures (Bell et al., 1998; Harmer and Gittins, 1998), provide support for formation by primary mantle melting while the association of alkaline igneous provinces with suture zones suggests carbonatites may be generated within the crust (Burke et al., 2003; Burke and Khan, 2006). Either scenario produces carbonate minerals crystallized at much higher temperatures than the sedimentary carbonates found abundantly on the Earth's surface and in deep-sea sediment cores.

Carbonatites are also thought to cool relatively rapidly. Haynes et al. (2003) assess the extent to which measured $\delta^{18}O$ values for calcite and associated silicate minerals from four carbonatites reflect isotopic compositions established during crystallization or, alternatively, diffusional exchange during cooling. They utilize the Fast Grain Boundary diffusion model (Eiler et al., 1992, 1993) to analyze retrograde diffusional exchange of oxygen isotopes between mineral grains for four different orders of magnitude cooling rates thought to be applicable to shallowly-intruded plutons (10^1, 10^2, 10^3, 10^4 °C per million years). Comparison of model results to oxygen isotope fractionations for

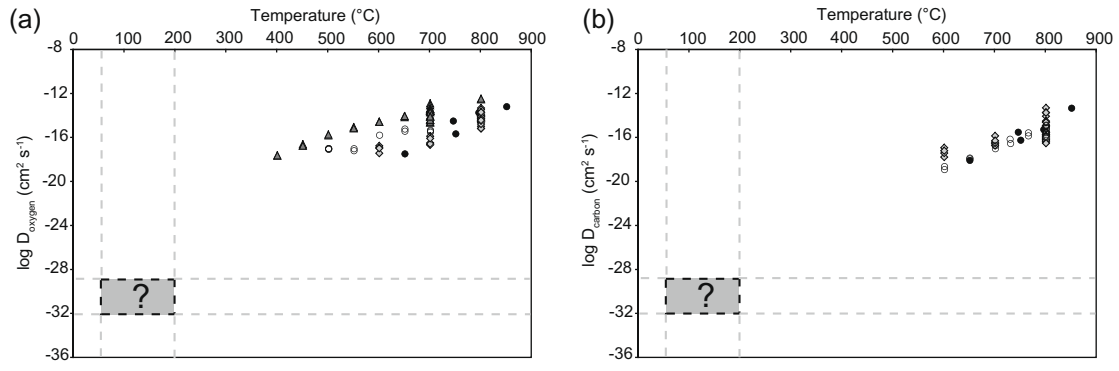

Fig. 1. Experimental results for the solid-state diffusion coefficients of oxygen (a) and carbon (b) in calcite. Data are from Farver (1994) (dark grey triangles), Kronenberg et al. (1984) (open circles), Labotka et al. (2004) (light grey diamonds), Anderson (1969, 1972) (black circles). The scatter in results for a given temperature is predominantly due to variable water content and pressure conditions. The grey boxes represent the range of diffusion coefficients that could be important on 10^6–10^9 year timescales for the clumped isotope paleothermometer.

calcite–silicate mineral pairs suggest most minerals measured, the exception being biotite, record temperatures within 100 °C of crystallization and indicated carbonatites crystallize over a range of temperatures from approximately 750 to 550 °C. This is consistent with the rapid cooling expected for small (km-scale) carbonatite plutons emplaced at shallow crustal depths. In comparison, deep-seated granite batholiths likely cool at slower rates (ca. 10 °C/my), and are more likely to record apparent closure temperatures rather than crystallization temperatures (Haynes et al., 2003).

The high temperature of crystallization and rapid cooling regime of carbonatites make the rocks suitable for a geologic test of the integrity of Δ_{47} in carbonate minerals. The primary high temperature signature of carbonatites is distinct from carbonates recording Earth's surface temperatures and therefore re-ordering of isotopologues due to solid-state diffusion and re-equilibration with burial or surface temperatures should be identifiable. A high temperature carbonate would be expected to fall below $\Delta_{47} = 0.35‰$ (corresponding to temperatures >200 °C when utilizing the theoretical calibration of Guo et al. (2009)), while a carbonate equilibrated at surface temperatures will fall into the range of 0.6–0.8‰ (corresponding to ca. 35–0 °C when utilizing the empirical calibration of Ghosh et al. (2006b)).

Due to the complex nature of carbonatite crystallization, we do not expect two carbonatites to yield the same clumped isotope signature. The sequential nucleation and growth of calcite and accessory carbonatite minerals occurs over a temperature interval corresponding to the liquidus and solidus, and while some phases with slow diffusion (e.g., diopside) will likely be closed to further exchange at sub-solidus temperatures, rapidly diffusing phases (e.g., biotite) may continue sub-solidus exchange of O with calcite (Haynes et al., 2003). The degree to which sub-solidus exchange continues is controlled by cooling rate, and could lead to different clumped isotope signatures between two carbonatites that crystallized at similar temperatures. The mineralogy of carbonatites can also vary due to the entrainment of country rock fragments, and the energetics of carbonatite crystallization, i.e., more passive intrusive conditions would allow the settling of silicate phases and dense mantle xenoliths, whereas extrusive conditions would likely entrain more silicate minerals from the surrounding country rock and prevent settling (Woolley and Church, 2005). Such variability in accessory mineral abundances could impact the clumped isotope signature by changing the minerals available for sub-solidus exchange with calcite, again resulting in two carbonatites crystallized at similar temperatures having different clumped isotope signatures. In summary, although carbonatite rocks crystallize at high temperatures and are predominantly composed of carbonate minerals, variability in the accessory mineralogy, intrusion depth, cooling regime and surface alteration will yield rocks with unique geochemical signatures. Therefore, variability in clumped isotope signatures of carbonatites, even without alteration, is expected.

Understanding that some variability in the clumped isotope signature of carbonatites is intrinsic to their complexity, it is possible to use the rocks as a test for the integrity of the clumped isotope proxy over 10^6–10^9 year timescales. By studying carbonatites, we address the following questions:

1. Do carbonatites retain a high temperature crystallization signature?
2. Does Δ_{47} become progressively heavier over time indicating loss of the primary clumped isotope signature and re-equilibration at lower temperatures, even when $\delta^{13}C$ and $\delta^{18}O$ indicate a pristine sample?
3. Is Δ_{47} recording the temperature of crystallization or the temperature at which exchange of C and O in the solid-state ceases during cooling?
4. Is Δ_{47} recording the temperature of dissolution and reprecipitation during metamorphic alteration of carbonatites?

2. METHODS

2.1. Samples

Carbonatite rock samples from 12 different sites of various ages and locations (Fig. 2) were obtained from the Division of Petrology and Volcanology, Department of Mineral Sciences, Smithsonian Institute (samples labeled NMNH-; Loan # 2045252 and Loan # 2048646), the Natural History Museum in London, UK (samples labeled BM-; Loan # 1370), Professor Nelson Eby at the University of Massachusetts-Amherst, and the Seaman Mineral Museum at Michigan Technological University (samples labeled SEA-; Loan # 8-06-08). Many of the sites have been studied using more than one rock sample (samples with different names for one site, e.g., OL-1c and BOK-7c), and within some hand samples, the sample has been drilled in multiple locations (samples with the same name, but different letters after the name, e.g., NMNH_116510-13, NMNH_116510-13-A and NMNH_116510-13-B).

The majority of samples are from intrusive igneous provinces, but Fort Portal (Barker and Nixon, 1989; Woolley, 2001; Bailey et al., 2005), Homa Mountain (Woolley, 2001) and Kaiserstuhl (Keller, 1981) are known to have extrusive activity. Although not all samples have been petrographically analyzed, those that record $\delta^{18}O$ signatures heavier than the primary igneous carbonatite range of 5.5–8.5‰ (V-SMOW) (Taylor et al., 1967; Keller and Hoefs, 1995) may be indicative of extrusive samples which have undergone low temperature weathering including exchange with meteoric water upon extrusion or equilibration with magmatic carbonatite waters at low temperatures (Deines and Gold, 1973). Three hand samples were identified as extrusive by their loaner: UG6 (lava), BM1998_P21_20 (lava), and NMNH_117180-17 (lapilli tuff). All samples have been measured for bulk stable isotopic compositions ($\delta^{13}C$ and $\delta^{18}O$) and clumped isotope signatures (Δ_{47}) as described in Section 2.3, with most samples being replicated at least three times to improve precision on Δ_{47}.

2.2. Inorganic precipitation experiments

In addition to the carbonatite samples, results are also presented for a Carrara marble lab standard and inorganic

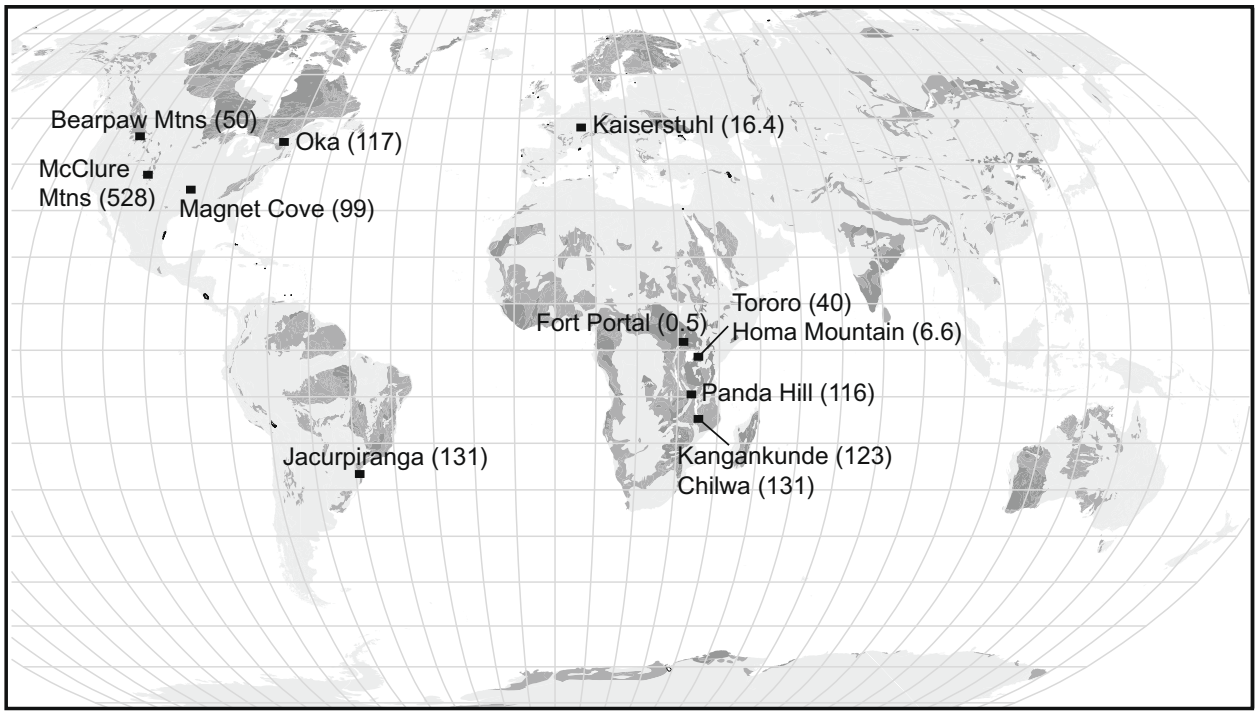

Fig. 2. Map (Woolley and Kjarsgaard, 2008) showing the location of the carbonatite suites analyzed in this study. The age of the carbonatite suites are in millions of years and shown in parentheses.

precipitation experiments. Inorganic $CaCO_3$ was precipitated at water bath controlled temperatures between 7.5 and 77 °C using a method akin to the passive degassing method (e.g., Kim et al., 2007). A 100 ml $CaCl_2$ solution was added to 900 ml solution of $NaHCO_3$, the concentrations of which were calculated using Geochemist's Workbench Release 5.0 to give a supersaturation with respect to calcite ($\Omega_{calcite}$) of approximately 10 once combined (Table 1). This saturation state was selected after preliminary work showed higher saturation states with faster precipitation resulted in isotopic disequilibrium.

The solutions were prepared by dissolving $NaHCO_3$ and $CaCl_2$ in separate beakers of deionized water that had been equilibrated to the desired water bath temperature for at least 2 h. Once dissolved, the $CaCl_2$ solution was slowly added in 5 ml quantities to the $NaHCO_3$ solution. The final solution remained un-sealed allowing equilibration and passive degassing to the atmosphere, and was continuously stirred for the duration of the experiment. Temperatures were controlled to within ±1 °C ($T < 50$ °C) or ±2 °C ($T \geqslant 50$ °C). Dependent on the temperature of the solutions, precipitation started after 2–24 h, and the solutions were filtered and air-dried after 1–4 days, to yield approximately 40 mg of $CaCO_3$. The precipitation experiments have been replicated at 15, 20, 30, and 70 °C. Note that due to slow initiation of precipitation (>3 days) for the repeat experiments at 15 and 30 °C, the saturation state of the solutions was increased to 19.4 and 13.7, respectively.

All inorganic $CaCO_3$ samples have been measured for bulk stable isotopic compositions ($\delta^{13}C$ and $\delta^{18}O$) and clumped isotope signatures (Δ_{47}). The oxygen isotopic composition of lab deionized water has also been analyzed via CO_2–H_2O equilibration at 25 °C.

2.3. Isotopic analysis of carbonates

The methodology used in the Laboratory for Geochemical Oceanography at Harvard University broadly follows that described in Eiler and Schauble (2004) and Ghosh et al. (2006b), but with minor modifications. Carbonate samples are prepared using a drill press and the bulk rock carbonate powder is weighed out into 15 mg samples. Some carbonatite rocks, due to their high silicate content have been sampled at up to 30 mg to ensure sufficient yield of CO_2 for analysis. Using a common acid bath with 90 °C phosphoric acid, powdered carbonate samples are acid digested and liberated CO_2 is collected by liquid nitrogen trapping after passing through a −80 °C ethyl alcohol water trap. Reaction time is on the order of 10 min, although for high silicate content carbonatites it can take up to 20 min for the reaction to proceed to completion.

All CO_2 samples are then passed through a PoraPak Q trap held at −10 °C using a glass vacuum line. PoraPak Q is a divinyl benzene polymer often used in a GC setup to separate hydrocarbons, but by packing a glass U-trap with PoraPak Q and using the pressure differential and pull of liquid nitrogen, the CO_2 samples flow through the static PoraPak Q trap without a carrier gas, while leaving any heavy hydrocarbons or chlorinated hydrocarbons attached to the trap (e.g., CH_3Cl, which can produce CCl^+ and $HCCl^+$ upon fragmentation and recombination during mass spectrometric analysis). The purified CO_2 stream is collected in a second U-trap on the far side of the PoraPak Q trap and active vacuum pumping ensures all CO_2 passed through trap is collected. After isolating the PoraPak Q trap, the CO_2 U-trap is allowed to warm and the CO_2 is transferred to a sample vial.

Table 1
Results for isotopic analysis of a Carrara marble standard (CM2) and the temperature-controlled inorganic $CaCO_3$ precipitation experiments. Analytical uncertainties for $\delta^{13}C$ (V-PDB), $\delta^{18}O$ (V-PDB) and Δ_{47} are shown as the standard error of the mean of all mass spectrometric analyses of a given sample. Also shown are the experimental conditions for the inorganic precipitation experiments, including the temperature of precipitation (T_{PPT}), the initial concentrations of $NaHCO_3$ and $CaCl_2$ solutions and the saturation state of the mixed solution with respect to calcite ($\Omega_{calcite}$). T_{KO97} gives the temperature calculated from the oxygen isotopic composition of the carbonate, lab deionized water ($\delta^{18}O = -36.48‰$ V-PDB) and the Kim and O'Neil (1997) calibration of the oxygen isotope thermometer. Repeat experiments have been conducted at 15, 20, 30 and 70 °C. See Section 4.1 for a discussion of the apparent disequilibrium precipitation for the repeat 30 °C experiment and at 70 and 77 °C.

CM2				n	$\delta^{13}C$ (‰)	$\delta^{18}O$ (‰)	Δ_{47} (‰)	
				53	2.26 ± 0.01	−1.80 ± 0.01	0.334 ± 0.004	
Inorganic $CaCO_3$								
T_{ppt} (°C)	$NaHCO_3$ (mM)	$CaCl_2$ (mM)	$\Omega_{calcite}$	n	$\delta^{13}C$ (‰)	$\delta^{18}O$ (‰)	Δ_{47} (‰)	T_{KO97} (°C)
7.5	3.7	43.7	10.8	2	−18.53 ± 0.02	−5.52 ± 0.16	0.656 ± 0.007	8.3
10	3.7	42.4	10.8	3	−17.69 ± 0.23	−5.83 ± 0.04	0.677 ± 0.006	9.7
15	3.5	40.0	10.7	2	−18.21 ± 0.11	−7.17 ± 0.06	0.649 ± 0.024	15.9
15	4.8	121.3	19.4	3	−15.59 ± 0.03	−6.88 ± 0.01	0.620 ± 0.015	14.5
20	3.4	37.4	10.6	2	−19.69 ± 0.11	−8.30 ± 0.08	0.629 ± 0.019	21.2
20	3.4	37.4	10.6	2	−19.16 ± 0.05	−8.09 ± 0.04	0.691 ± 0.028	20.2
25	3.4	37.5	10.6	2	−19.38 ± 0.10	−9.24 ± 0.10	0.640 ± 0.004	25.9
30	3.1	34.9	10.7	3	−19.17 ± 0.06	−10.04 ± 0.01	0.608 ± 0.014	29.9
30	3.1	59.6	13.7	2	−14.82 ± 0.03	−9.57 ± 0.06	0.612 ± 0.002	27.5
40	2.8	32.5	10.6	4	−18.93 ± 0.04	−11.99 ± 0.03	0.586 ± 0.014	40.3
50	2.4	30.0	10.7	5	−18.31 ± 0.04	−13.55 ± 0.07	0.549 ± 0.014	49.1
60	2.2	27.5	11.4	4	−16.79 ± 0.67	−15.21 ± 0.08	0.562 ± 0.015	59.2
70	1.9	24.9	10.8	4	−16.58 ± 0.11	−15.48 ± 0.07	0.530 ± 0.008	60.8
70	1.9	24.9	10.8	3	−13.11 ± 0.55	−15.18 ± 0.04	0.555 ± 0.019	59.0
77	1.7	22.5	11.3	3	−17.99 ± 0.11	−16.94 ± 0.10	0.526 ± 0.015	70.3

The purified CO_2 samples are analyzed on a Thermo Finnigan MAT 253 for $\delta^{13}C$, $\delta^{18}O$ and Δ_{47}. The dual inlet IRMS is configured to measure mass 44 through 48 CO_2 through the following resistors: mass $44 = 3 \times 10^7\ \Omega$, mass $45 = 3 \times 10^9\ \Omega$, mass $46 = 1 \times 10^{10}\ \Omega$, mass $47 = 1 \times 10^{12}\ \Omega$, mass $48 = 1 \times 10^{12}\ \Omega$. The amplification of the doubly-substituted mass 47 and mass 48 ion beams allows the IRMS to run at sufficiently high voltages to achieve stable mass 47 and 48 measurements, while avoiding saturation of the ions beams of higher abundance masses 44 through 46 CO_2. Data is acquired by balancing at 8 V on mass 47, with masses 44, 45, 46 and 48 registering at approximately 5, 5.5, 6.5 and 0.7 V. The equivalent currents are 0.17 μA, 2 nA, 0.65 nA, 8 pA, 0.7 pA for masses 44 through 48, respectively. A CO_2 sample is measured for one acquisition comprised of 20 counts with one standard-sample-standard cycle per count. Ion integration time is 26 s per change-over (520 s of total current integration time) and the bellows are pressure adjusted between each count. Individual samples run for approximately 2 h on the IRMS. For typical measurement protocol, the shot-noise limit to precision is 0.009‰ (Merritt and Hayes, 1994).

Minor modifications have been made to the MAT 253, including the addition of 5 ml dead volumes between the bellows and capillaries, and a change in capillaries from stainless steel to 110 μm deactivated fused-silica capillaries. The dead volume was added to decrease the change in gas pressure (and therefore voltage) during a single standard-sample-standard cycle, and the deactivated fused-silica capillaries were installed to prevent exchange between CO_2 and H_2O within the capillaries.

Carbonate and CO_2 gas standards are also run every 2–3 days to monitor machine drift and correct for variable bulk isotopic compositions and non-linearities in the source. As with previous clumped isotope studies (e.g., Eiler and Schauble, 2004; Huntington et al., 2009), the IRMS used in this study exhibits measurable non-linearities between CO_2 gas samples known to have the same clumped isotope composition. This process is quantified by preparing quartz break-seals of CO_2 gas standards with variable bulk isotopic composition, and heating these samples to 1000 °C for 2 h in a muffle furnace. After heating, the break-seals are quenched to room temperature and hence maintain the stochastic distribution of isotopologues achieved at 1000 °C. When analyzed, we find heated gases of variable bulk isotopic composition exhibit subtle differences in their clumped isotope composition. The relationship between bulk isotopic composition (δ^{47}) and clumped isotope composition (Δ_{47}) is linear over the range of gas standards measured ($\delta^{47} = -41.7$–$16.3‰$), but the slope and intercept can shift over periods of months. Therefore, all data generated for carbonate samples are corrected back to a common bulk isotopic composition using the slope of the heated gas line at the time of their measurement. The regression of Δ_{47} onto δ^{47} yields a slope from 0.0043 to 0.0053, and intercepts from −0.9636 to −0.9244 between September 2008 and December 2009. Changes in the intercept of the heated gas line over time likely reflect isotopic 'scrambling' due to fragmentation and recombination of isotopologues in the source (Huntington et al., 2009), and are corrected by scaling all data to a fixed intercept. We have selected this intercept as the intercept of the heated

gas line over the time of the inorganic precipitation experiments (Δ_{47}[HG vs. WG] = −0.9244‰). The corrections employed in this study are the same as those discussed in detail by Huntington et al. (2009).

In addition to the CO_2 heated gas standards, a Carrara marble carbonate standard is run before and after approximately every 20 carbonatite samples. This standard can be used to identify any problems with sample preparation, such as leaks during acid digestion or on the vacuum line, and background contaminants as measured by the mass 48 signal. Until further inter-lab comparisons can be made, the Carrara marble standard is also used as a proxy for an inter-lab standard.

3. RESULTS

3.1. Standards and inorganic precipitation experiments

A Carrara marble standard (CM2) has been measured in replicate since January 2009 and yields $\Delta_{47} = 0.334 \pm 0.004$‰ (1$\sigma$ standard error; $n = 53$). Run to run reproducibility is therefore equal to 0.029‰ (1σ), while internal counting statistics are 0.012 (1σ standard error), closely approaching the shot-noise limit of 0.009‰. The results of inorganic precipitation experiments are shown in Table 1 and Fig. 3. The correction for acid digestion at 90 °C applied to this Δ_{47} data, and all data going forward, is based on Eq. 23 of Guo et al. (2009). Clumped isotope signatures for inorganic precipitates range from 0.526‰ to 0.691‰, or 56.1 to 15.4 °C, respectively, when using the original calibration (Ghosh et al., 2006b; Eq. (2)). $\delta^{13}C$ ranges from −19.69‰ to −13.11‰ (V-PDB) and $\delta^{18}O$ ranges from −16.94‰ to −5.52‰ (V-PDB).

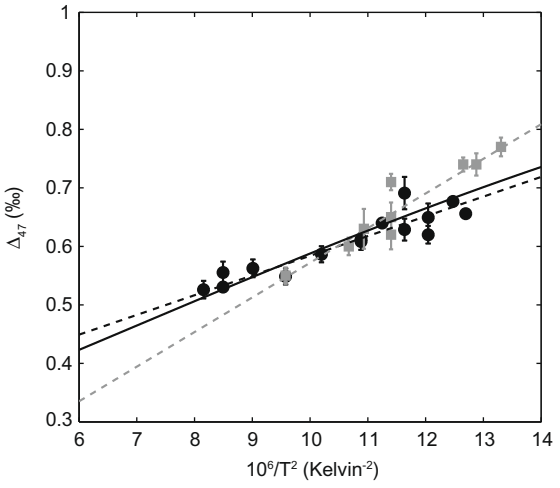

Fig. 3. Inorganic calibration of the clumped isotope proxy. Grey squares show the original calibration by Ghosh et al. (2006b), and the dashed grey line is Eq. (2) derived from the Ghosh et al. (2006b) data. The solid black line is the theoretical calibration given in Eq. (3) (Guo et al., 2009). The black circles are data from the inorganic calibration performed in this study. Linear regression of this data yields the black dashed line ($R^2 = 0.9074$). Error bars denote the standard error of the mean of all mass spectrometric analyses of a given sample. Note that $CaCO_3$ precipitated during the repeat 30 °C experiment and at 70 and 77 °C may have precipitated in disequilibrium, although removing these data points from the linear regression still yields a regression within error of Eq. (4).

3.2. Carbonatites

Results for the analysis of carbonatite samples are presented in Table 2, which shows the bulk isotopic composition ($\delta^{13}C$ and $\delta^{18}O$), the clumped isotope signature (Δ_{47}), and the temperature corresponding to the Δ_{47} value of a given sample. An empirical calibration has not been conducted at high temperatures (above ca. 70 °C), therefore temperatures in Table 2 are calculated using the theoretical relationship between Δ_{47} and temperature for calcite given in Eq. 18 of Guo et al. (2009). Due to the non-linear dependence of Δ_{47} on temperature, analytical uncertainties equate to larger temperature errors at crustal temperatures (Eiler et al., 2009), and therefore temperatures shown in Table 2 should be viewed as order of magnitude signals.

Table 2 shows variability between and within the different carbonatite sites and Δ_{47} ranges from 0.275‰ to 0.545‰ (or approximately 416 and 61 °C, respectively). $\delta^{13}C$ ranges from −10.0‰ to −2.3‰ (V-PDB) and $\delta^{18}O$ ranges from 6.9‰ to 19.0‰ (V-SMOW). Samples from Fort Portal, Uganda (0.5 Ma) give clumped isotope signatures of 0.275‰ and 0.501‰ (416 and 83 °C). Homa Mountain, Kenya (6.6 Ma) samples range in Δ_{47} from 0.312‰ to 0.421‰ (284–137 °C) with a median of 0.364‰. Kaiserstuhl, Germany (16 Ma) samples range in Δ_{47} from 0.322‰ to 0.545‰ (264–61 °C) with a median of 0.358‰. The carbonatite sample from Tororo, Uganda (40 Ma) gives a clumped isotope signature of 0.362‰ (198 °C). Samples from Bearpaw Mountains, MT (50 Ma) range from 0.406‰ to 0.489‰ (150–90 °C) with a median of 0.442‰. The Magnet Cove, AK (99 Ma) carbonatite yields a clumped isotope signature of 0.420‰ (138 °C). The sample from Panda Hill, Tanzania (116 Ma) gives 0.309‰ (293 °C). Samples from Oka, Canada (117 Ma) range in Δ_{47} from 0.342‰ to 0.398‰ (228–157 °C) with a median of 0.375‰. The carbonatite sample from Kangankunde, Malawi (123 Ma) yields a clumped isotope signature of 0.439‰ (123 °C). The Jacupiranga, Brazil (131 Ma) samples yields $\Delta_{47} = 0.402$‰ (153 °C). The sample from Chilwa, Malawi (131 Ma) gives a clumped isotope signature of 0.428‰ (131 °C). And, the sample from McClure Mountains, CO (528 Ma) has a Δ_{47} signature of 0.438‰ (124 °C). Standard errors of the mean of all mass spectrometric analyses of a given sample range from 0.001‰ to 0.040‰ (median = 0.012‰) with only 6 out of the 45 samples run giving a standard error greater than 0.015‰.

Bulk recrystallization via fluid–rock interaction and post-depositional alteration is identified in carbonatite samples by comparing the oxygen isotopic composition of a given sample to its clumped isotope signature. Fig. 4 illustrates the relationship between $\delta^{18}O$ and Δ_{47} for four sites with replicate samples (Homa Mountain, Kaiserstuhl, Bearpaw Mountains and Oka). The plot shows a positive correlation between $\delta^{18}O$ and Δ_{47} for samples from Homa Mountain, Kenya and Kaiserstuhl, Germany with $\delta^{18}O$

Table 2
Results for carbonatite analysis showing sample location, age (Ma), number of repeat analyses of a given sample, $\delta^{13}C$ (V-PDB), $\delta^{18}O$ (V-SMOW), Δ_{47} and temperature (°C) calculated from Δ_{47}. Carbonatite ages are from Woolley and Kjarsgaard (2008). The average standard errors on $\delta^{13}C$ and $\delta^{18}O$ are 0.03‰ and 0.09‰, respectively. Analytical uncertainties in Δ_{47} are shown in the table as the standard error of the mean of all mass spectrometric analyses of a given sample. Temperature is calculated using the theoretical relationship between temperature and Δ_{47} for calcite given in Guo et al. (2009). Samples identified by loaner as extrusive are marked, as are those that have been excluded from Fig. 5 based on evidence of contamination or alteration.

Sample	Location	Age	*n*	$\delta^{13}C$ (‰)	$\delta^{18}O$ (‰)	Δ_{47} (‰)	*T* (°C)
UG6[a,c]	Fort Portal, Uganda	0.5	5	−9.6	18.4	0.501 ± 0.012	83
BM1998_P21_20[a,c]	Fort Portal, Uganda	0.5	5	−8.4	10.1	0.275 ± 0.026	416
NMNH_110903	Homa Mountain, Kenya	6.6	5	−3.4	7.9	0.332 ± 0.011	244
NMNH_110903-A	Homa Mountain, Kenya	6.6	3	−3.6	7.7	0.312 ± 0.004	284
NMNH_110903-B	Homa Mountain, Kenya	6.6	3	−3.4	7.7	0.365 ± 0.040	194
NMNH_110903-C	Homa Mountain, Kenya	6.6	3	−3.4	8.4	0.364 ± 0.007	196
NMNH_110915	Homa Mountain, Kenya	6.6	4	−3.6	8.6	0.354 ± 0.011	208
NMNH_110915-A	Homa Mountain, Kenya	6.6	3	−3.1	9.4	0.421 ± 0.013	137
NMNH_110915-B	Homa Mountain, Kenya	6.6	3	−3.2	9.2	0.388 ± 0.018	167
NMNH_110915-C	Homa Mountain, Kenya	6.6	3	−3.2	9.2	0.373 ± 0.003	184
NMNH_116510-13	Kaiserstuhl, Germany	16	6	−5.7	7.1	0.355 ± 0.013	206
NMNH_116510-13-A	Kaiserstuhl, Germany	16	3	−5.9	7.6	0.360 ± 0.015	201
NMNH_116510-13-B	Kaiserstuhl, Germany	16	3	−5.7	7.2	0.327 ± 0.011	253
NMNH_117180-6	Kaiserstuhl, Germany	16	5	−5.7	7.1	0.355 ± 0.014	207
NMNH_117180-6-A	Kaiserstuhl, Germany	16	3	−5.7	7.0	0.329 ± 0.008	249
NMNH_117180-6-B	Kaiserstuhl, Germany	16	3	−5.7	7.0	0.331 ± 0.013	247
NMNH_117180-13	Kaiserstuhl, Germany	16	8	−6.2	7.8	0.322 ± 0.013	264
NMNH_117180-13-A	Kaiserstuhl, Germany	16	3	−6.4	8.6	0.348 ± 0.011	217
NMNH_117180-13-B	Kaiserstuhl, Germany	16	3	−6.2	7.7	0.340 ± 0.012	230
NMNH_117180-15[c]	Kaiserstuhl, Germany	16	3	−6.8	11.5	0.389 ± 0.014	167
NMNH_117180-15-A[c]	Kaiserstuhl, Germany	16	3	−7.0	13.1	0.441 ± 0.021	121
NMNH_117180-15-B[c]	Kaiserstuhl, Germany	16	3	−6.5	10.8	0.398 ± 0.004	158
NMNH_117180-17[b,c]	Kaiserstuhl, Germany	16	3	−10.0	18.6	0.518 ± 0.007	74
NMNH_117180-17-A[b,c]	Kaiserstuhl, Germany	16	3	−9.2	16.9	0.450 ± 0.011	114
BM1992-P2(9)[c]	Kaiserstuhl, Germany	16	4	−10.0	19.0	0.545 ± 0.006	61
BM1992-P2(9)-A[c]	Kaiserstuhl, Germany	16	3	−9.5	18.2	0.539 ± 0.014	69
NMNH_109369-21	Tororo, Uganda	40	4	−3.2	7.3	0.362 ± 0.005	198
NMNH_117247-194	Bearpaw Mountains, MT	50	6	−7.6	8.6	0.426 ± 0.013	133
NMNH_117247-194-A	Bearpaw Mountains, MT	50	3	−7.5	8.8	0.407 ± 0.028	149
NMNH_117247-194-B	Bearpaw Mountains, MT	50	2	−7.6	9.0	0.465 ± 0.003	104
NMNH_117247-194-C	Bearpaw Mountains, MT	50	3	−7.4	8.9	0.443 ± 0.012	119
NMNH_117247-194-D	Bearpaw Mountains, MT	50	3	−7.4	9.0	0.441 ± 0.019	121
NMNH_117216-209[c]	Bearpaw Mountains, MT	50	4	−7.9	8.7	0.489 ± 0.007	90
NMNH_117216-209-A	Bearpaw Mountains, MT	50	2	−8.2	8.3	0.406 ± 0.010	150
NMNH_117216-209-B	Bearpaw Mountains, MT	50	3	−8.3	8.3	0.453 ± 0.010	112
MC3	Magnet Cove, AK	99	5	−5.2	8.7	0.420 ± 0.011	138
NMNH_109369-49	Panda Hill, Tanzania	116	5	−4.3	8.5	0.309 ± 0.015	293
OL-1c	Oka, Canada	117	3	−5.3	6.9	0.385 ± 0.014	170
BOK-6c	Oka, Canada	117	3	−5.8	7.1	0.398 ± 0.013	157
BOK-7c	Oka, Canada	117	3	−5.2	7.1	0.342 ± 0.002	228
BOK-7	Oka, Canada	117	3	−5.2	7.3	0.365 ± 0.007	195
NMNH_109369-38	Kangankunde, Malawi	123	4	−2.3	8.5	0.439 ± 0.013	123
SEA-JAC	Jacupiranga, Brazil	131	5	−6.1	7.4	0.402 ± 0.014	153
NMNH_109369-37	Chilwa, Malawi	131	4	−2.9	7.9	0.428 ± 0.012	131
SEA-MCC	McClure Mountains, CO	528	4	−7.4	7.4	0.438 ± 0.001	124

[a] Identified by loaner as lava.
[b] Identified by loaner as lapilli tuff.
[c] Excluded from Fig. 5 due to evidence of contamination or alteration.

ranging from 7.7‰ to 9.4‰ and 7.0‰ to 19.0‰, respectively. No such correlation exists for samples from Bearpaw Mountains or Oka and these sites have variability in $\delta^{18}O$ of less than 1‰. Samples from Bearpaw Mountains, MT range in $\delta^{18}O$ from 8.3‰ to 9.0‰, while those from Oka, Canada range from 6.9‰ to 7.3‰,

4. DISCUSSION

4.1. Standards and inorganic precipitation experiments

An Italian marble has also been measured by Ghosh et al. (2006b) and yields 0.341 ± 0.019‰, or 0.007‰ heavier than

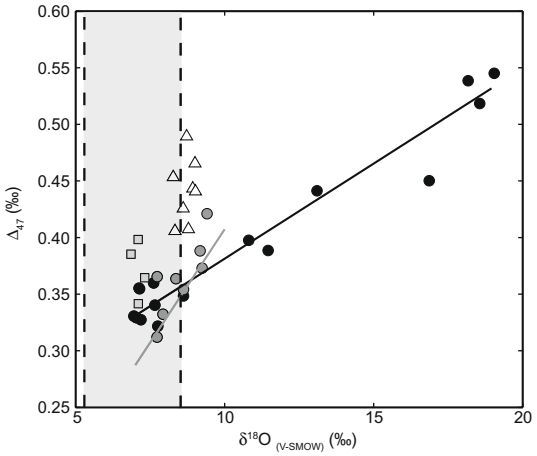

Fig. 4. Plot showing the relationship between $\delta^{18}O$ and Δ_{47} at the four sites where multiple samples were analyzed. The light grey shading encompasses the $\delta^{18}O$ field denoted by Taylor et al. (1967) and Keller and Hoefs (1995) as primary igneous carbonatites ($\delta^{18}O = 5.5–8.5‰$). Samples are from Kaiserstuhl, Germany (black circles), Homa Mountain, Kenya (dark grey circles), Bearpaw Mountains, MT (light grey triangles), and Oka, Canada (grey squares). The R^2 values for linear regressions of Δ_{47} onto $\delta^{18}O$ for Kaiserstuhl (black line) and Homa Mountain (grey line) are 0.970 and 0.887, respectively.

the signature of CM2 measured here ($\Delta_{47} = 0.334 \pm 0.004‰$). Carrara marble is used here as a gross measure of inter-lab reproducibility, but labs measuring clumped isotopes are also developing a full set of inter-lab working standards. This network of standards will better enable labs to work in the same reference frame, use the same calibration curves and directly cross-correlate results.

The results of inorganic precipitation experiments shown in Table 1 and Fig. 3 deviate from the original calibration curve (Ghosh et al., 2006b; Eq. (2)) at temperatures below 20 and above 60 °C. Linear regression of the inorganic precipitation data generated here yields the following relationship between Δ_{47} and temperature (Kelvin) with a R^2 value of 0.9074:

$$\Delta_{47} = \frac{(0.0337 \pm 0.0018) \times 10^6}{T^2} + (0.2470 \pm 0.0194) \qquad (4)$$

Also shown in Fig. 3 is the theoretical calibration of the clumped isotope thermometer for calcite corrected for acid digestion at 90 °C (Eqs. 18 and 23 of Guo et al. (2009)). This theoretical calibration closely aligns the data generated in this study. Although the results shown suggest the slope of the calibration could be shallower than initially predicted by Ghosh et al. (2006b) (Eq. (2)), extensive analysis of modern natural carbonates continue to fall on the original calibration curve (Eiler et al., 2009), therefore continued use of the original calibration for natural carbonates precipitated between 1 and 50 °C is justified. For higher temperature carbonates, such as the carbonatites measured here, the theoretical calculation of Guo et al. (2009) is the most appropriate calibration. Again, these discrepancies in calibration curves point to the need for an inter-lab set of standards.

Two possible explanations for deviations from the original calibration of Ghosh et al. (2006b) include (i) material precipitated was not single-phase calcite, but also included aragonite and amorphous carbonate and (ii) precipitation proceeded out of isotopic equilibrium with water. First, the precipitates were not analyzed by XRD, therefore we cannot be certain of mineralogy and deviations in slope may be attributable to changes in carbonate phase, especially as theoretical studies predict small offsets in the clumped isotope signature of calcite, aragonite and other metal-carbonates at equal precipitation temperature (Schauble et al., 2006; Guo et al., 2009). Second, to test for equilibrium precipitation the isotopic composition of the carbonates and the deionized water from which the carbonate precipitated was compared to the oxygen isotope paleothermometer of Kim and O'Neil (1997) (Table 1).

CO_2–H_2O equilibration of lab deionized water at 25 °C yields $\delta^{18}O = -36.48‰$ (V-PDB). Using this oxygen isotopic composition of water, inorganic precipitates have $\delta^{18}O_{carbonate}$ signatures within ±1.2 °C of that expected for the Kim and O'Neil (1997) thermometer, with the exception of inorganic $CaCO_3$ precipitated at 70 and 77 °C, and the repeat precipitation experiment at 30 °C. The repeat precipitation experiment at 30 °C is heavier by 2.5 °C (ca. 0.5‰) and was precipitated under high calcite saturation ($\Omega_{calcite} = 13.7$), while the inorganic carbonates precipitated at 70 and 77 °C are heavier than expected by 7–11 °C (ca. 1.4–2.2‰). Disequilibrium may have occurred due to insufficient pre-equilibration of the initial $NaHCO_3$ solution, and therefore these inorganic carbonates could have inherited the isotopic composition of the $NaHCO_3$ powder. We consider this unlikely as all carbonates were prepared by the same method, and for the majority of the inorganic carbonates, disequilibrium precipitation does not appear to be the reason for discrepancies between Eq. (4) and the initial calibration of Ghosh et al. (2006b) (Eq. (2)). It may be appropriate to give lower confidence to the results above 70 °C based on oxygen isotope disequilibrium, although removing them from the data set produces a regression within error of Eq. (4).

The 15, 30 and 70 °C repeat precipitation experiments were conducted approximately 2–3 months after the first round of experiments, were much slower to precipitate (>24 h) and yielded less $CaCO_3$. The repeat experiments at 15 and 30 °C were also those that required higher saturation states to precipitate carbonate ($\Omega_{calcite} = 19.4$ and 13.7, respectively). We conjecture that changing laboratory conditions, including increasing humidity and temperature, due to the experiments being conducted in August, compared to May and early June, may explain these discrepancies. These three repeat experiments yield heavier carbon isotope signatures than the initial $CaCO_3$ precipitated at the same temperature, but the clumped isotope signature was reproduced to within the standard errors of replicate analyses. This is possible because Δ_{47} is a measure of the deviation in mass 47 CO_2 from that expected from a sample's bulk stochastic distribution. Therefore, any two carbonates precipitated at the same temperature should yield the same Δ_{47} value, even if $\delta^{13}C$ varies.

Finally, another possible explanation for discrepancies between the inorganic precipitation study of Ghosh et al. (2006b) and this study could be inter-lab differences in sample preparation and IRMS analysis. Although raw clumped isotope data is corrected in the same way as that of other labs (Huntington et al., 2009), further inter-lab comparisons are required to fully understand if differences between labs are due to precipitation experiments, samples preparation or isotopic analysis. This work is ongoing among the labs conducting clumped isotope research, and includes the measurement of samples with known clumped isotopic compositions and CO_2 gas standards.

4.2. Carbonatites

Sample contamination and the bulk isotopic composition of carbonatite samples can explain some of the variability in Δ_{47} (Table 2). For example, the two samples from Fort Portal, Uganda (UG6 and BM1998_P21_20) have been excluded from further discussion because of contamination and evidence of post-depositional alteration. Sample BM1998_P21_20 is designated contaminated because of the high mass 48 voltages associated with the sample, poor reproducibility on Δ_{47} (standard error of 5 mass spectrometric analyses is ±0.026‰) and a visibly high silicate content (slow reaction time upon acid digestion and residual silicate remaining in the acid bath). Several mass spectrometric analyses of BM1998_P21_20 yielded mass 48 voltages greater than 5 V and memory effects in the source suggest the contaminant is sulfur (e.g., recombinations yielding $^{32}S^{16}O$ in the source). The second sample from Fort Portal, UG6, is excluded from further discussion based on its bulk stable isotopic composition ($\delta^{13}C = -9.6‰$ and $\delta^{18}O = 18.4‰$) which falls outside of the primary igneous carbonatite field defined as $\delta^{13}C = -8.0‰$ to $-5.0‰$ and $\delta^{18}O = 5.5–8.5‰$ (Taylor et al., 1967; Keller and Hoefs, 1995). This sample has likely undergone post-depositional alteration and therefore Δ_{47} will not be recording the primary clumped isotope signature.

Bulk recrystallization of carbonatites is assessed by a cross-plot of $\delta^{18}O$ and Δ_{47} (Fig. 4). Data from the four sites with multiple samples analyzed (Kaiserstuhl, Homa Mountain, Bearpaw Mountains and Oka) show a positive correlation between $\delta^{18}O$ and Δ_{47} when samples depart from the primary igneous carbonatite range. The correlation ($R^2 = 0.970$) is most apparent for Kaiserstuhl carbonatites which range from $\delta^{18}O = 7‰$ and $\Delta_{47} = 0.32‰$ to $\delta^{18}O = 19‰$ and $\Delta_{47} = 0.55‰$. A similar correlation is present in Homa Mountain samples, but the slope is steeper when Δ_{47} is regressed onto $\delta^{18}O$ and its significance lower ($R^2 = 0.887$). Samples from Bearpaw Mountains and Oka show variability in Δ_{47} on the order of 0.07‰ with little change in $\delta^{18}O$, and the bulk isotopic composition of these samples predominantly fall into the primary igneous carbonatite range. Six samples from Bearpaw Mountains fall outside of the $\delta^{18}O$ primary igneous carbonatite field by up to 0.5‰, but we do not consider alteration as the cause because no positive correlation exists between $\delta^{18}O$ and Δ_{47}. An exception is sample NMNH_117216-209 which has a heavy Δ_{47} value of 0.489 while still retaining a light oxygen isotopic composition at $\delta^{18}O = 8.7‰$. High mass 48 voltage readings for this sample suggest a contaminated sample, and it is excluded it from further discussion.

Using the criteria discussed above, Fig. 5 shows the clumped isotope signature of samples with no evidence for broad-scale fluid-rock interaction ($\delta^{18}O < 10‰$) plotted against the age of the carbonatite. The data covers much of the past 150 Ma and shows no clear trend towards heavier Δ_{47} with increasing age, although there is significant variability in the clumped isotope signature both between and within sites.

Results for pristine carbonatites (Fig. 5) indicate the clumped isotope proxy is not recording the formation or crystallization temperature of the carbonatites, but instead the temperature at which isotope exchange ceases during cooling. The lightest Δ_{47} values recorded, samples NMNH_110903-A from Homa Mountain at 0.312 ±

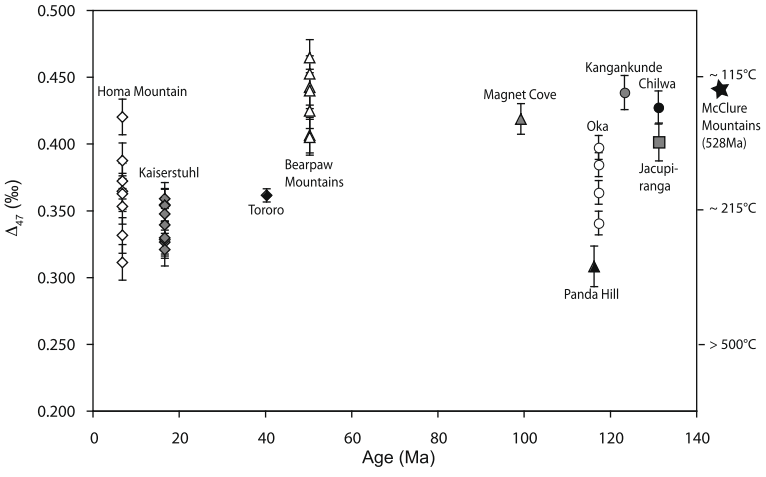

Fig. 5. Clumped isotope signature of well-preserved carbonatite samples plotted against the age of that given carbonatite suite. Error bars denote the average standard error of the mean of all mass spectrometric analyses of a given carbonatite site. The McClure Mountains carbonatite, with an age of 528 Ma, has been plotted to the right of the figure in line with its Δ_{47} value. Using the temperature–Δ_{47} relationship of Guo et al. (2009), the approximate temperatures inferred from $\Delta_{47} = 0.250‰$, 0.350‰ and 0.450‰ are shown on the right *y*-axis.

0.004‰ and NMNH_109369-49 from Panda Hill at 0.309 ± 0.015‰, correspond to temperatures no greater than 293 °C, and are significantly lower than the temperatures of carbonatite crystallization. Similarly, the Carrara marble standard, a pristine metamorphosed carbonate, records a temperature of 241 °C ($\Delta_{47} = 0.334 \pm 0.004$‰). This suggests the temperature at which solid-state exchange ceases is in the range of 250–300 °C, and that these temperatures may represent an upper limit on temperatures recorded by the clumped isotope proxy in natural carbonates. This result aligns with earlier work suggesting an apparent 'blocking temperature' for slowly cooled marbles at ~200 °C and evidence for intracrystalline isotope exchange resulting in partial re-equilibration at temperatures ⩽350 °C (Eiler et al., 2009).

Although solid-state diffusion may be controlling the exchange of isotopes above this temperature, there is no systematic trend in the clumped isotopic signature of the pristine carbonatites with age (Fig. 5). Some of the older samples (e.g., NMNH_109369-38 from Kangankunde, Malawi) record temperatures only in the range of 120 °C implying closed system re-equilibration at burial temperatures may have occurred, while other samples, also from the Lower Cretaceous (e.g., NMNH_109369-49 from Panda Hill, Tanzania and BOK-7c from Oka, Canada) record temperatures above 200 °C. The oldest sample, SEA-MCC from the Early Paleozoic McClure Mountains in Colorado, records a Δ_{47} signature of 0.438 ± 0.001‰, or approximately 120 °C. It is not possible to base a conclusion on this one data point in the Early Paleozoic, but it suggests re-equilibration to progressively heavier clumped isotopic signatures, without bulk alteration, is not occurring even over a 0.5×10^9 year timescale. Even so, re-equilibration can occur if a sample has been exposed to burial temperatures for long periods of time. This implies solid-state diffusion of O or C atoms within the carbonate lattice is sufficiently slow to enable the use of Δ_{47} on 10^8 year timescales, but that caution should be used when interpreting temperature data from samples exposed to burial temperatures for millions of years.

Fission track data helps in understanding the cooling regime and minimum ages of igneous rocks, and is used here to interpret clumped isotope signatures. Mean apatite fission track data represent the time when a rock cools through 100 ± 20 °C, the closure temperature for fission track retention in apatite. For the Oka carbonatite, apatite fission track data give a mean age of 122 Ma, coinciding with other age constraints for Oka of 109–120 Ma from K–Ar, Rb–Sr and U–Pb (Lentz et al., 2006). The fission track data suggests the complex has not been exposed to burial metamorphism since its emplacement, cooled relatively rapidly and/or that the intrusion temperature was relatively low (Gold et al., 1986). Our analysis gives Δ_{47} values from 0.342‰ to 0.398‰ (ca. 230–150 °C) implying that the complex has not continued slow re-equilibration to Earth's surface temperatures since being emplaced in the Mid-Cretaceous and, in conjunction, with the fission track data we can also rule out the signature being acquired during a closed-system burial metamorphism event.

Apatite fission track data can also be used to better understand the clumped isotope signature of the McClure Mountains complex. The McClure Mountain alkalic complex, which is cut by carbonatite dikes, intruded into lower Proterozoic metamorphic granitic and hornblende gneisses and amphibolites in the early Cambrian (Lynnes and Van Der Voo, 1984; Woolley, 1987), with K–Ar and Rb–Sr dating techniques giving ages ranging from 535 to 506 Ma (Woolley, 1987). Apatite fission track dates give a much younger age of 293 ± 62 Ma (Lynnes and Van Der Voo, 1984), suggesting alteration of the complex occurred ca. 300 Ma. The clumped isotope signature of SEA-MCC from the McClure Mountains is 0.438‰ (ca. 120 °C), a temperature that aligns with the apatite fission track closure temperature, and suggests that solid-state diffusion has not been playing an important role in controlling the clumped isotope signature since approximately 300 Ma.

Although solid-state diffusion does not lead to a systematic trend in Δ_{47} with age, carbonatites record different degrees of clumping. The scatter in Δ_{47} among and between sites (Fig. 5) suggests there is variability in the temperature at which a clumped isotope signature is retained. Such variability could be explained by differences in cooling regimes, water content and the rock's mineralogy and silica content. If cooling were fast, the clumped isotope signature should record a higher temperature, whereas if cooling were slow, exchange could continue over longer periods of time and at lower temperatures. For example, sample NMNH_109369-37 from Chilwa Island, Malawi ($\Delta_{47} = 0.428 \pm 0.012$‰) records a heavy clumped isotope signature in comparison to many other carbonatites measured. Fission track data and field assessments suggest the complex at Chilwa Island was emplaced shallowly in the crust and that it cooled slowly with a residence time of ca. 60 my in the apatite partial annealing zone (the zone which corresponds to a range in temperature from 130 to 60 °C for apatite fission tracks) (Eby et al., 1995). This implies slow cooling results in carbonatites recording heavier clumped isotope signatures than carbonatites that cool quickly.

Other factors may also be important in determining a carbonatite's clumped isotope signature. For example, higher water contents will likely translate into faster exchange of O isotopes, and therefore lower temperature clumped isotope signatures, and variable mineralogy and silica contents will also likely impact clumped isotope signature.

5. CONCLUSION

Inorganic $CaCO_3$ precipitation experiments have been conducted and provide a second calibration for the clumped isotope paleothermometer over the range of 7.5–77 °C. The calibration aligns with a recent theoretical calculation of acid fractionation associated with the carbonate clumped isotope thermometer, but discrepancies exist between our results and the original calibration (Ghosh et al., 2006b). Work is ongoing to develop an inter-lab comparison of clumped isotope standards that may help to explain this discrepancy.

Carbonatites have been used as a geologic test for the integrity of the clumped isotope proxy over greater than 10^7 year timescales. Carbonatites of various ages ranging

from recent to the Early Paleozoic retain different clumped isotope signatures, but those considered well preserved, based on their $\delta^{18}O$, show no trend in Δ_{47} with age. This suggests re-equilibration to Earth's surface temperatures is not occurring over time, although re-equilibration to burial temperatures can occur if a carbonatite has been exposed to greater than approximately 100 °C for millions of years. None of the high temperature carbonates measured record signatures lighter than 0.31‰, implying isotope exchange continues during cooling until ca. 250–300 °C. Even excluding carbonatites that have undergone post-depositional open-system exchange of oxygen, there is considerable variability in the clumped isotope signature of carbonatites. This is likely due to differences in mineralogy, water content, cooling rate and burial history. In conclusion, the solid-state reordering of O and C atoms is sufficiently slow to enable the use of clumped isotope paleothermometry on timescales of 10^8 years, although we encourage caution when interpreting temperature data from samples exposed to burial temperatures for long periods of time.

ACKNOWLEDGMENTS

This work was supported by Henry and Wendy Breck. Samples were kindly provided by the Division of Petrology and Volcanology, Department of Mineral Sciences, Smithsonian Institute (Loan # 2045252 and Loan # 2048646), the Natural History Museum in London, UK (Loan # 1370), Professor Nelson Eby at the University of Massachusetts-Amherst, and the Seaman Mineral Museum at Michigan Technological University (Loan # 8-06-08). The authors thank John Eiler for suggestions, comments and discussion on clumped isotope geochemistry, and a thoughtful review. The authors thank James Farquhar for his editorial handling of this manuscript and two anonymous reviewers for insightful and constructive comments. The authors also thank John Higgins and Itay Halevy for in-lab discussions and suggestions, and Greg Eischeid, Clara Blättler and Renata Cummins for laboratory assistance.

REFERENCES

Affek H. P., Bar-Matthews M., Ayalon A., Matthews A. and Eiler J. M. (2008) Glacial/interglacial temperature variations in Soreq cave speleothems as recorded by 'clumped isotope' thermometry. *Geochim. Cosmochim. Acta* **72**(22), 5351–5360.

Anderson T. F. (1969) Self-diffusion of carbon and oxygen in calcite by isotope exchange with carbon dioxide. *J. Geophys. Res.* **74**(15), 3918–3932.

Anderson T. F. (1972) Self-diffusion of carbon and oxygen in dolomite. *J. Geophys. Res.* **77**(5), 857–861.

Bailey K., Lloyd F., Kearns S., Stoppa F., Eby N. and Woolley A. (2005) Melilitite at Fort Portal, Uganda: another dimension to the carbonate volcanism. *Lithos* **85**(1–4), 15–25.

Barker D. S. and Nixon P. H. (1989) High-Ca, low-alkali carbonatite volcanism at Fort-Portal, Uganda. *Contrib. Mineral. Petrol.* **103**(2), 166–177.

Bell K., Kjarsgaard B. A. and Simonetti A. (1998) Carbonatites – into the twenty-first century. *J. Petrol.* **39**(11–12), 1839–1845.

Burke K. and Khan S. (2006) Geoinformatic approach to global nepheline syenite and carbonatite distribution: testing a Wilson cycle model. *Geosphere* **2**(1), 53–60.

Burke K., Ashwal L. D. and Webb S. J. (2003) New way to map old sutures using deformed alkaline rocks and carbonatites. *Geology* **31**(5), 391–394.

Came R. E., Eiler J. M., Veizer J., Azmy K., Brand U. and Weidman C. R. (2007) Coupling of surface temperatures and atmospheric CO_2 concentrations during the Palaeozoic era. *Nature* **449**(7159), 198–201.

Deines P. and Gold D. P. (1973) Isotopic composition of carbonatite and kimberlite carbonates and their bearing on isotopic composition of deep-seated carbon. *Geochim. Cosmochim. Acta* **37**(7), 1709–1733.

Eby G. N., Rodentice M., Krueger H. L., Ewing W., Faxon E. H. and Woolley A. R. (1995) Geochronology and cooling history of the northern part of the Chilwa Alkaline Province, Malawi. *J. Afr. Earth Sci.* **20**(3–4), 275–288.

Eiler J. M. (2007) "Clumped-isotope" geochemistry – the study of naturally-occurring, multiply-substituted isotopologues. *Earth Planet. Sci. Lett.* **262**(3–4), 309–327.

Eiler J. M. and Schauble E. (2004) O-18–C-13–O-16 in Earth's atmosphere. *Geochim. Cosmochim. Acta* **68**(23), 4767–4777.

Eiler J. M., Baumgartner L. P. and Valley J. W. (1992) Intercrystalline stable isotope diffusion – a fast grain-boundary model. *Contrib. Mineral. Petrol.* **112**(4), 543–557.

Eiler J. M., Valley J. W. and Baumgartner L. P. (1993) A new look at stable-isotope thermometry. *Geochim. Cosmochim. Acta* **57**(11), 2571–2583.

Eiler J. M., Boniface M. and Daeron M. (2009) 'Clumped isotope' thermometry for high-temperature problems. *Geochim. Cosmochim. Acta* **73**(13), A322.

Farver J. R. (1994) Oxygen self-diffusion in calcite – dependence on temperature and water fugacity. *Earth Planet. Sci. Lett.* **121**(3–4), 575–587.

Ghosh P., Garzione C. N. and Eiler J. M. (2006a) Rapid uplift of the Altiplano revealed through C-13–O-18 bonds in paleosol carbonates. *Science* **311**(5760), 511–515.

Ghosh P., Adkins J., Affek H., Balta B., Guo W. F., Schauble E. A., Schrag D. and Eller J. M. (2006b) C-13–O-18 bonds in carbonate minerals: a new kind of paleothermometer. *Geochim. Cosmochim. Acta* **70**(6), 1439–1456.

Gittins J. (1979) Problems inherent in the application of calcite–dolomite geothermometry to carbonatites. *Contrib. Mineral. Petrol.* **69**(1), 1–4.

Gold D. P., Eby G. N., Bell K. and Vallee M. (1986) Field Trip 21: Carbonatites, Diatremes, and Ultra-Alkaline Rocks in the Oka Area, Quebec. *Geological Association of Canada, Mineralogical Association of Canada, Canadian Geophysical Union, Joint Annual Meeting.*

Guo W. and Eiler J. M. (2007) Temperatures of aqueous alteration and evidence for methane generation on the parent bodies of the CM chondrites. *Geochim. Cosmochim. Acta* **71**(22), 5565–5575.

Guo W. F., Mosenfelder J. L., Goddard W. A. and Eiler J. M. (2009) Isotopic fractionations associated with phosphoric acid digestion of carbonate minerals: insights from first-principles theoretical modeling and clumped isotope measurements. *Geochim. Cosmochim. Acta* **73**(24), 7203–7225.

Harmer R. E. and Gittins J. (1998) The case for primary, mantle-derived carbonatite magma. *J. Petrol.* **39**(11–12), 1895–1903.

Haynes E. A., Moecher D. P. and Spicuzza M. J. (2003) Oxygen isotope composition of carbonates, silicates, and oxides in selected carbonatites: constraints on crystallization temperatures of carbonatite magmas. *Chem. Geol.* **193**(1–2), 43–57.

Huntington K. W., Eiler J. M., Affek H. P., Guo W., Bonifacie M., Yeung L. Y., Thiagarajan N., Passey B., Tripati A., Daeron M. and Came R. (2009) Methods and limitations of 'clumped' CO_2 isotope (Delta(47)) analysis by gas-source isotope ratio mass spectrometry. *J. Mass Spectrom.* **44**(9), 1318–1329.

Keller J. (1981) Carbonatitic volcanism in the Kaiserstuhl alkaline complex – evidence for highly fluid carbonatitic melts at the Earths surface. *J. Volcanol. Geoth. Res.* **9**(4), 423–431.

Keller J. and Hoefs J. (1995) Stable isotope characteristics of recent natrocarbonatites from Oldoinyo Lengai. In *Carbonatite Volcanism: Oldoinyo Lengai and the Petrogenesis of Natrocarbonatites*, vol. 4 (eds. K. Bell and J. Keller). Springer-Verlag, pp. 113–123.

Kim S. T. and O'Neil J. R. (1997) Equilibrium and nonequilibrium oxygen isotope effects in synthetic carbonates. *Geochim. Cosmochim. Acta* **61**(16), 3461–3475.

Kim S. T., O'Neil J. R., Hillaire-Marcel C. and Mucci A. (2007) Oxygen isotope fractionation between synthetic aragonite and water: influence of temperature and Mg^{2+} concentration. *Geochim. Cosmochim. Acta* **71**(19), 4704–4715.

Kronenberg A. K., Yund R. A. and Giletti B. J. (1984) Carbon and oxygen diffusion in calcite – effects of Mn content and Ph2o. *Phys. Chem. Mineral.* **11**(3), 101–112.

Labotka T. C., Cole D. R., Riciputi L. R. and Fayek M. (2004) Diffusion of C and O in calcite from 0.1 to 200 MPa. *Am. Mineral.* **89**(5–6), 799–806.

Lentz D., Eby N., Lavoie S. and Park A. (2006) Field Trip B4: Diatremes, Dykes and Diapirs: Revisiting the Ultra-Alkaline to Carbonatitic Magmatism of the Monteregian Hills. *Geological Association of Canada, Mineralogical Association of Canada, Joint Annual Meeting*.

Lynnes C. S. and Van der Voo R. (1984) Paleomagnetism of the Cambro-Ordovician Mcclure mountain alkalic complex, Colorado. *Earth Planet. Sci. Lett.* **71**(1), 163–172.

Merritt D. A. and Hayes J. M. (1994) Factors controlling precision and accuracy in isotope-ratio-monitoring mass-spectrometry. *Anal. Chem.* **66**(14), 2336–2347.

Schauble E. A., Ghosh P. and Eiler J. M. (2006) Preferential formation of C-13–O-18 bonds in carbonate minerals, estimated using first-principles lattice dynamics. *Geochim. Cosmochim. Acta* **70**(10), 2510–2529.

Taylor H. P., Frechen J. and Degens E. T. (1967) Oxygen and carbon isotope studies of carbonatites from the Laacher See District, West Germany and the Alno District, Sweden. *Geochim. Cosmochim. Acta* **31**(3), 407–430.

Woolley A. R. (1987) *Alkaline Rocks and Carbonatites of the World. Part 1: North and South America*. British Museum (Natural History).

Woolley A. R. (2001) *Alkaline Rocks and Carbonatites of the World. Part 3: Africa*. The Geological Society.

Woolley A. R. and Church A. A. (2005) Extrusive carbonatites: a brief review. *Lithos* **85**(1–4), 1–14.

Woolley A. R. and Kjarsgaard B. A. (2008) Carbonatite occurrences of the world: map and database. In *Open File 5796*. Geological Survey of Canada.

Associate editor: James Farquhar